Atmospheric Phase

Copies of slides are on the teaching tab of my physics web pages

https://www.physics.ox.ac.uk/our-people/rochep/teaching

Atmospheric Refraction

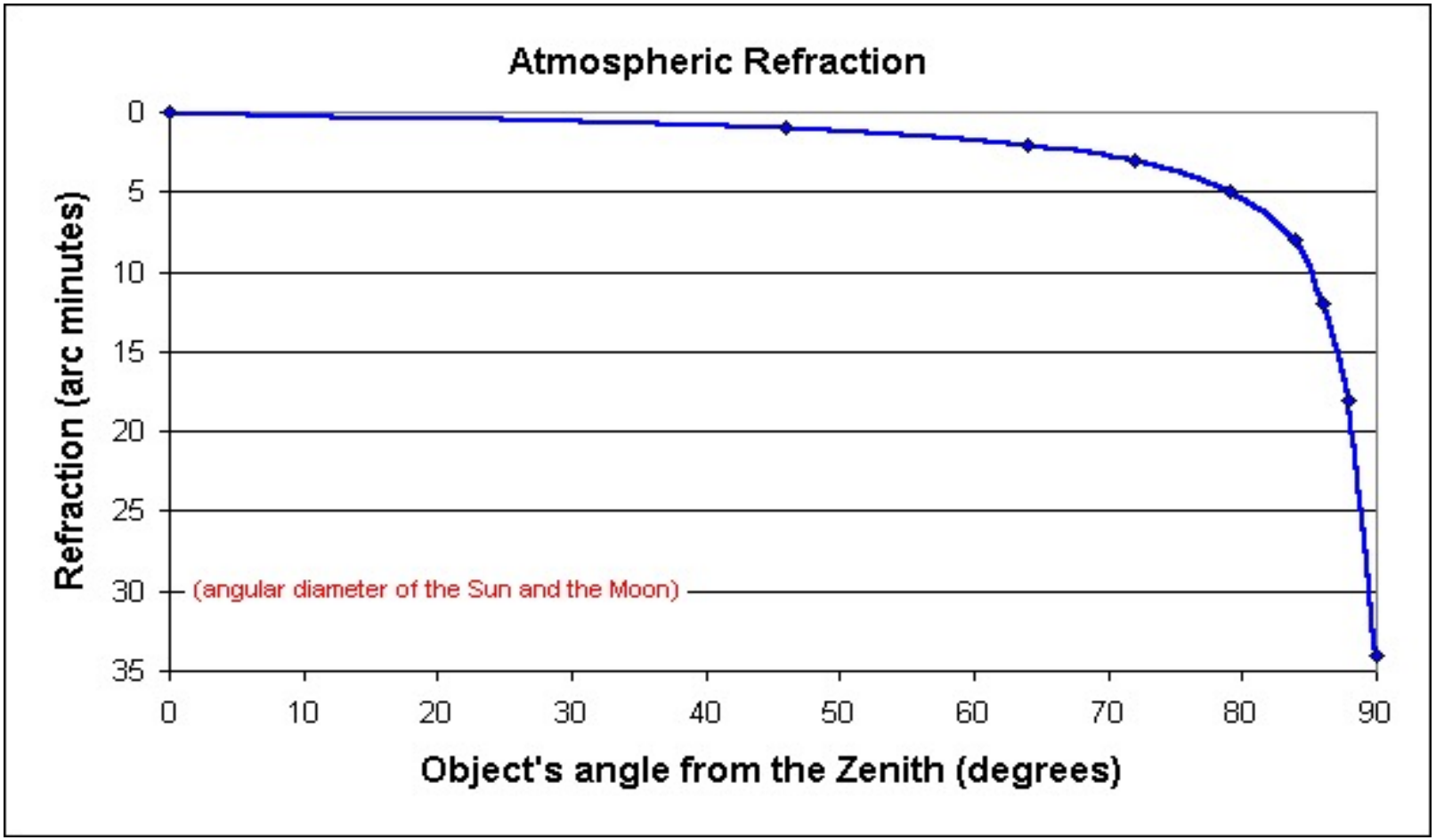

- Observations made away from the zenith pass through atmospheric layers at an angle, leading to increasing refraction with zenith distance.

Refraction at different atmospheric layers

- Refraction at different atmospheric layers
- Accurate values require a full atmospheric model, taking account of P,T and n at different elevations

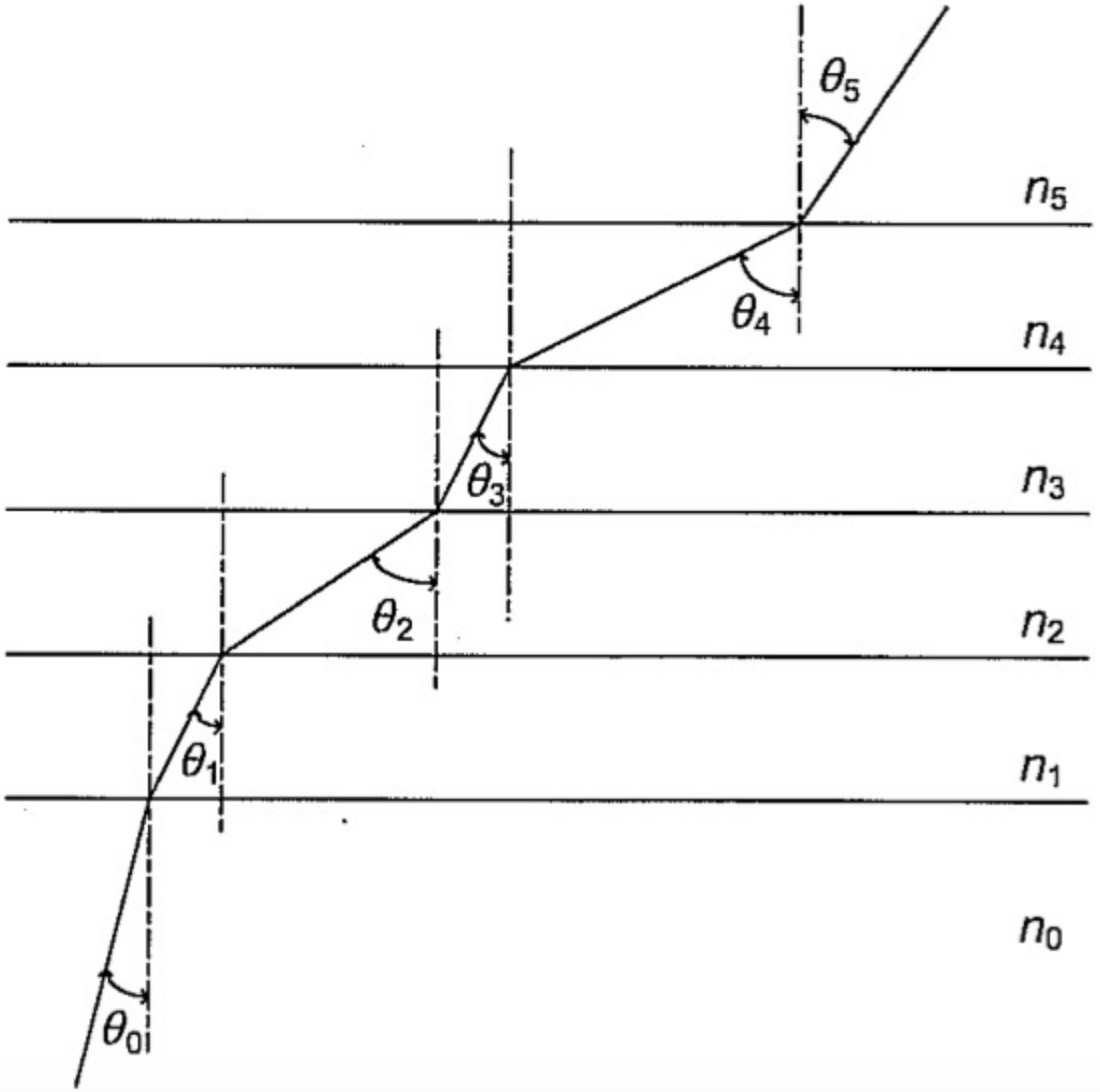

Atmospheric Refraction at Mauna Kea			
Zenith angle, degrees	Mauna Kea Table, arc seconds	Conventional theory, arc seconds	Lihue data, arc seconds
45^o	36.70	36.80	36.81
50^o	43.72	43.83	43.84
55^o	52.35	52.47	52.50
60^o	63.41	63.54	63.59
65^o	78.35	78.48	78.56
70^o	100.0	100.1	100.2
75^o	134.7	134.7	135.0
80^o	200.0	199.6	200.6
85^o	361.8	361.6	366.5

TABLE OF ATMOSPHERIC REFRACTION AT THE MAUNA KEA OBSERVATORY, FOR $\lambda = .633$ MICRONS. THE FIRST COLUMN ARE OBSERVATIONS ANGLES RELATIVE TO THE OBSERVER'S ZENITH. THE SECOND COLUMN IS A REFRACTION TABLE AT THE MAUNA KEA OBSERVATORY. THE THIRD COLUMN WAS CALCULATED FROM THE CONVENTIONAL PARAMETERS. THE FOURTH COLUMN WAS CALCULATED FROM A LEAST SQUARES FIT TO THE LIHUE DATA FOR THE RATIO PRESSURE/TEMPERATURE DEPENDENCE ON ALTITUDE. IN KAUAI, ON AUGUST 20,2016.

M Nauenberg 2016

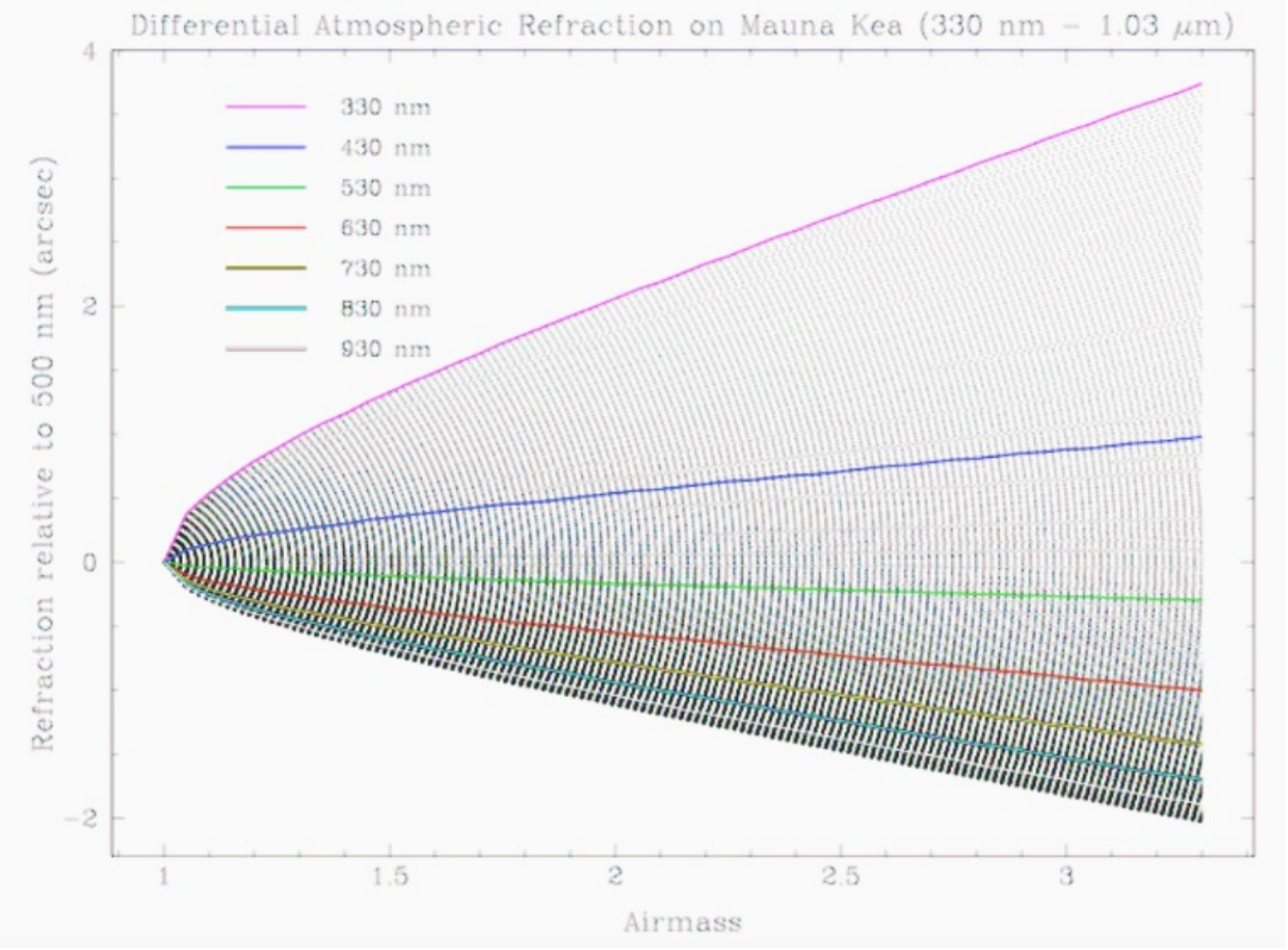

The atmospheric refractive index increases with decreasing wavelength so that blue wavelengths suffer greater refraction than red, leading to dispersion. Dispersion increases rapidly with zenith distance. The plot shows the dispersion as sec(Z) ranges from 1.1 to 3 airmass (Gemini GMOS web pages)

Differential atmospheric refraction effects are more pronounced at shorter wavelengths and under good seeing conditions.

The effect of differential atmospheric refraction (relative to 500 nm) on Mauna Kea (model) for a point source image with disk seeing of 0.3" and at three different airmasses (1.05, 1.5 and 2.0)

Observations in the g' filter (wavelength range 398-552 nm): the model star looks strongly elongated, particularly at airmasses 1.5 and 2

The effects are much lower in the IR, but may be important for wide-field IR instruments with AO correction

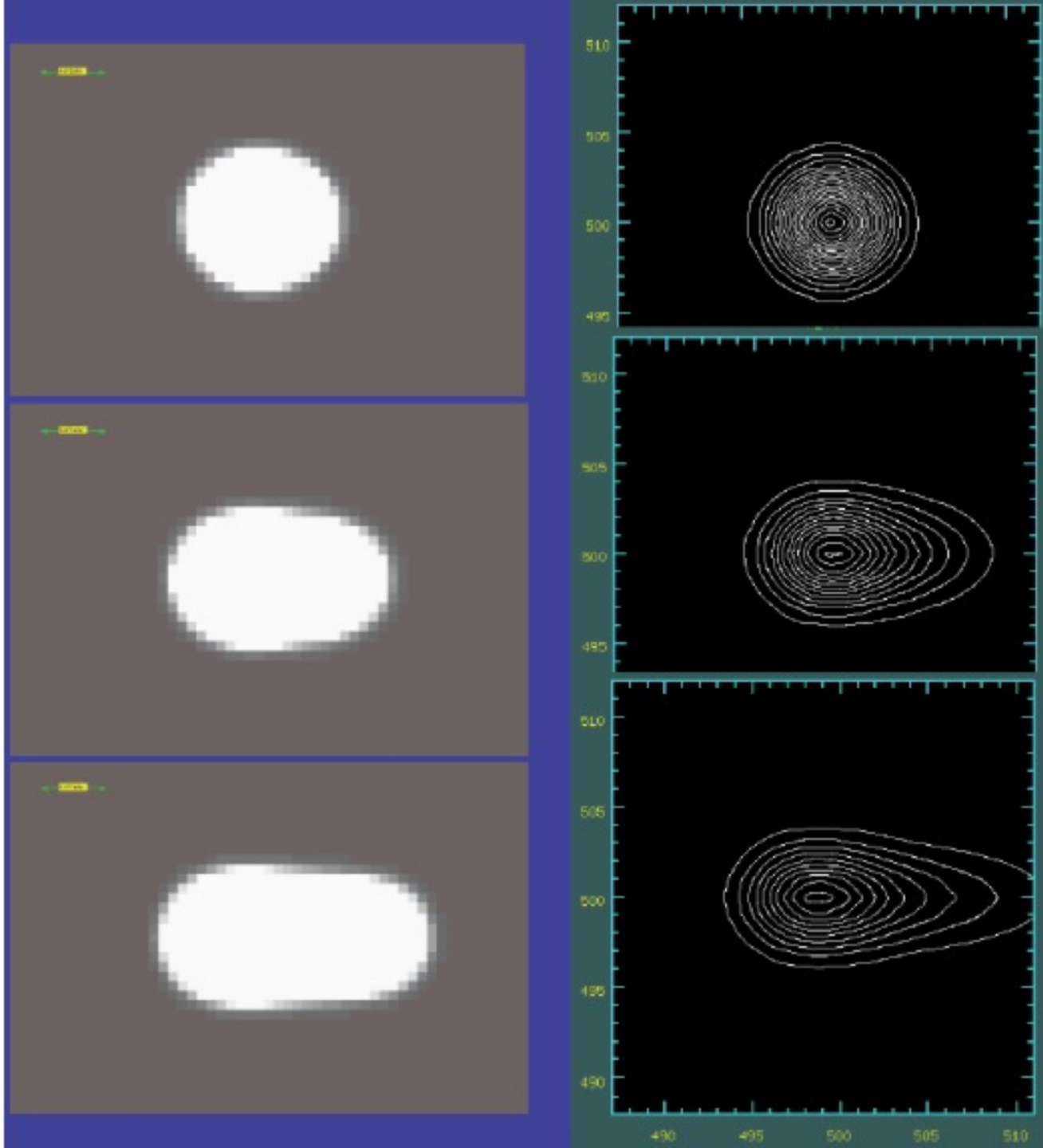

Parallactic Angle for Mauna Kea:

Latitude 19^{o} 45’ N

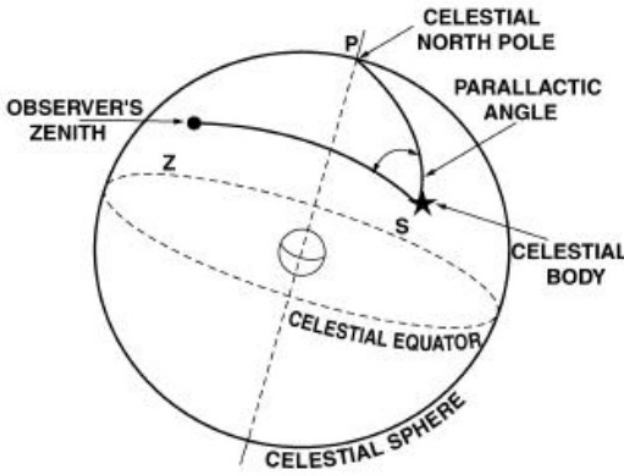

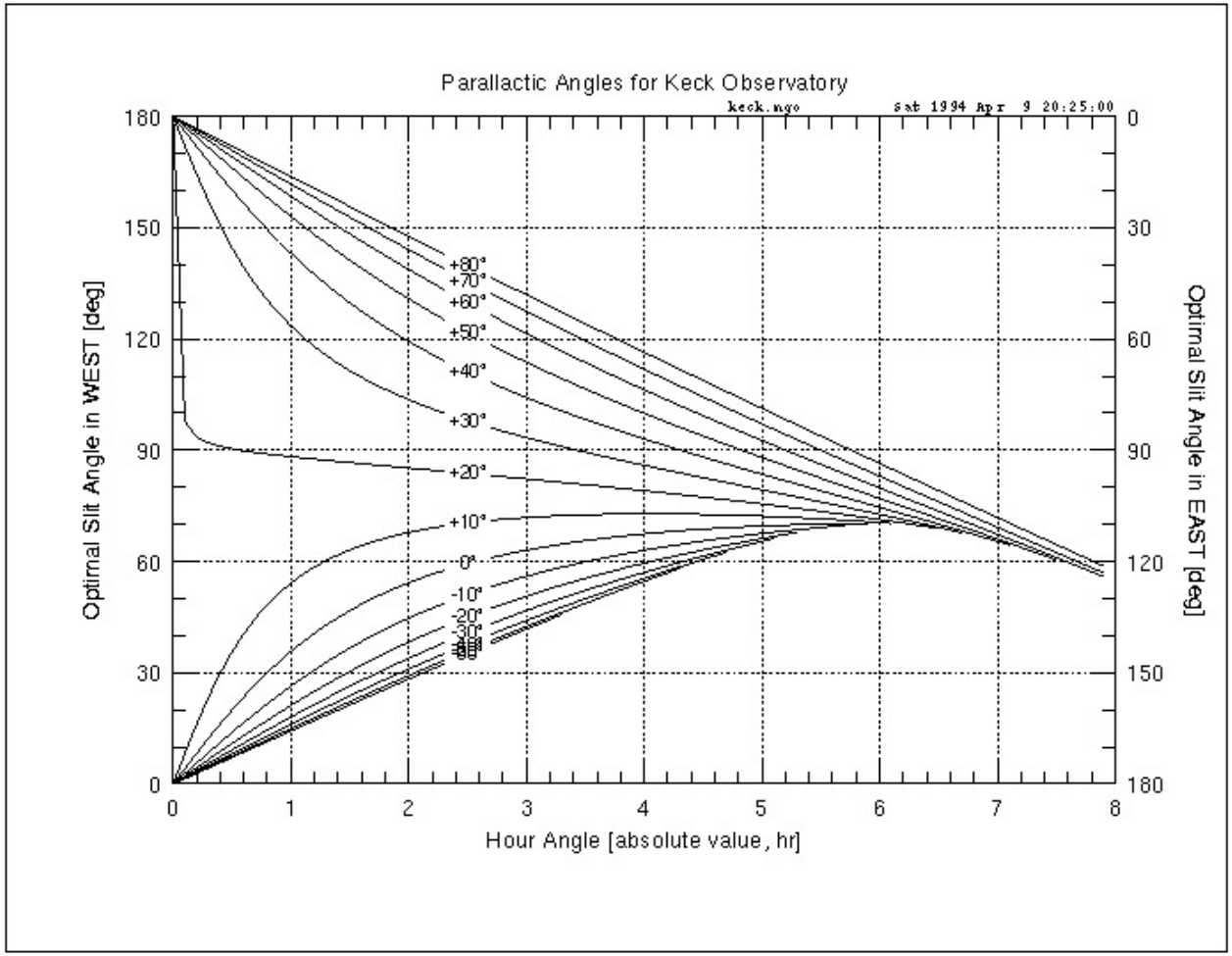

The local vertical angle with respect to North at a particular Declination and Hour Angle

Atmospheric Dispersion Correction

- Many imagers incorporate an Atmospheric Dispersion compensator (a pair of prisms that can be rotated to compensate for dispersion optically)
- Even then, differential refraction and dispersion across the field of wide field instruments may be significant
- Improved image quality and narrow slits require more accurate refraction compensation.
- Careful attention to slit angles is needed to ensure that all wavelengths are admitted by a slit – observations may need to be made at the parallactic angle

Differential Refraction at Paranal

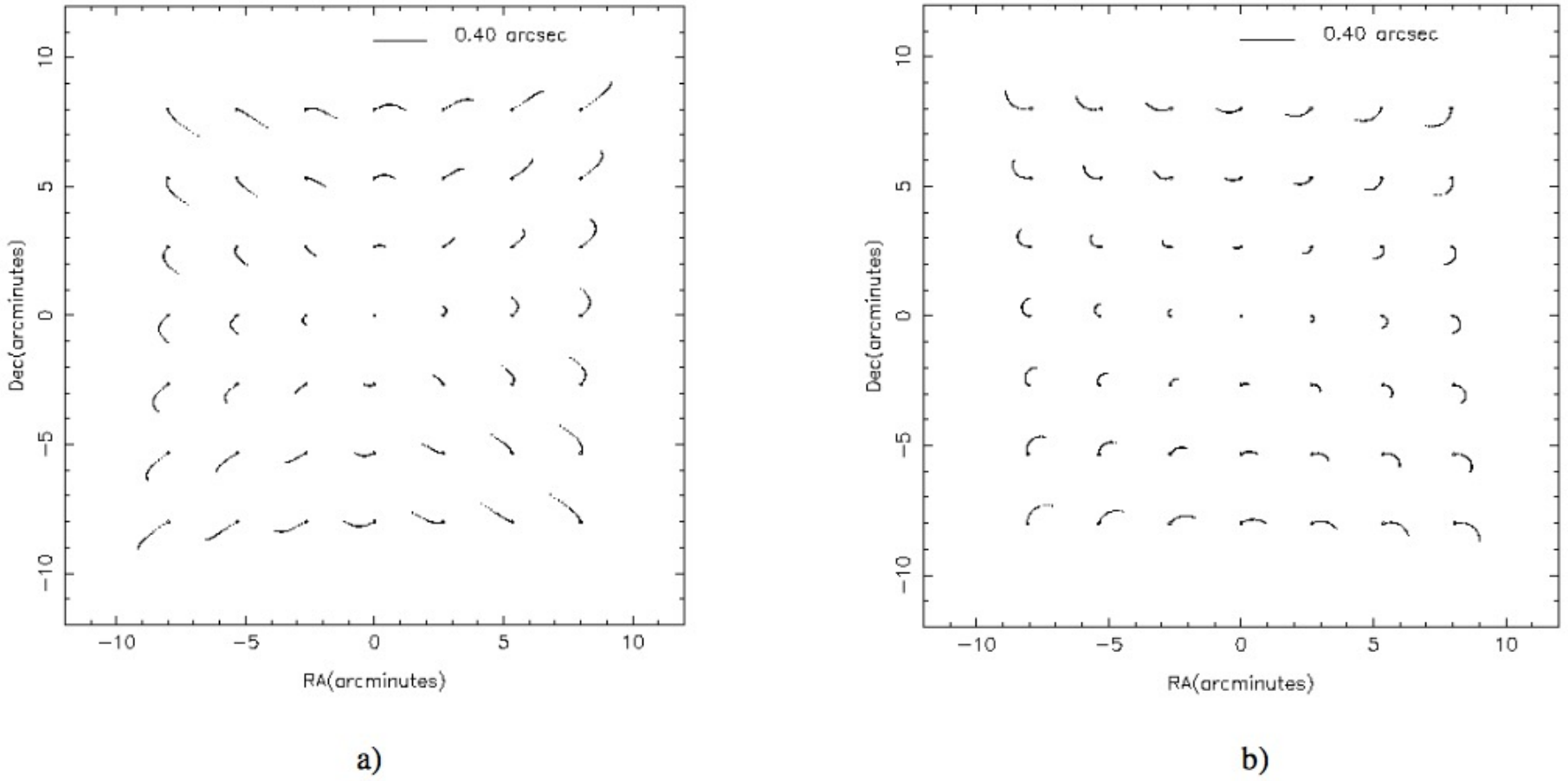

Figure 1. Field differential refraction for a 4 hour exposure starting -2 hours from meridian: a) for a northern object at a +25° declination; b) for a southern objetc at a -75° declination

The figure shows the differential refraction after field rotation has been compensated for a 16 x 16 arcmin field on Paranal, e.g. for the VIMOS instrument. (J-G Cuby et al)

Wide-field spectroscopy

- Observations with Multi-Object spectrographs in the visible have particular requirements that may affect observation planning
  - Differential refraction across the field changes the mean position of objects over an integration
  - Dispersion is minimised by tracking the parallactic angle
  - But the field on an alt-az telescope rotates
- Some compromise may be needed.
  - Integrations may be split over several nights so that the range of Hour Angle (and thus Parallactic angle variation) is reduced
  - For very wide-field instruments, different slit masks or fibre positions may be needed for observations at different Hour Angles
- Much more detailed treatment of these issues can be found in instrument handbooks or e.g. (Newman P.R. 2002 PASP 114 918).

Radio Frequencies

- λ <3cm water vapour absorption – need high dry sites
- Between 3cm-50cm atmosphere has little effect on observations (except high winds)
- λ >50cm ionosphere and solar activity impact observations - observations at night are preferred
- Refraction in the troposphere:
  - n_{air}= 1.00029 at T=0°C and P=760mm of Hg
  - At radio frequencies water vapour increases dielectric constant and has a substantial effect on the refractive index
  - Effect is the same as at shorter wavelengths, but dispersion is not significant
  - Refractive delay is an important factor in interferometry

Refractive delay

The delay caused by propagation through the atmosphere is the integral of the refractive index along the path

$$t = \int_{r_0}^{\infty} \frac{n(r)}{\sec(z)} dr$$

In practice in interferometry, what matters is the differential delay between different telescopes or antennas.

At IR wavelengths, this can amount to many wavelengths, but for most radio telescopes, Δt is rather small

The figure shows contours of delay as a function of baseline and elevation. The contours are 10, 15, 20, 25, 50, 75, 100, 200, 400, 600, 800, 1000, 3000, and 5000 μm from right to left

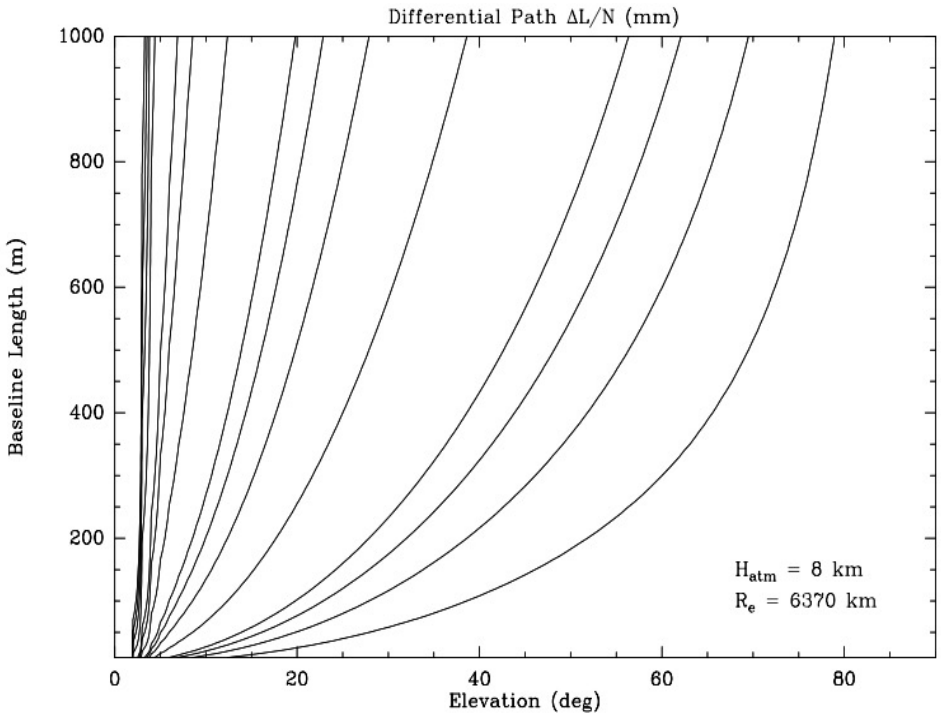

Interferometer Geometric Delay

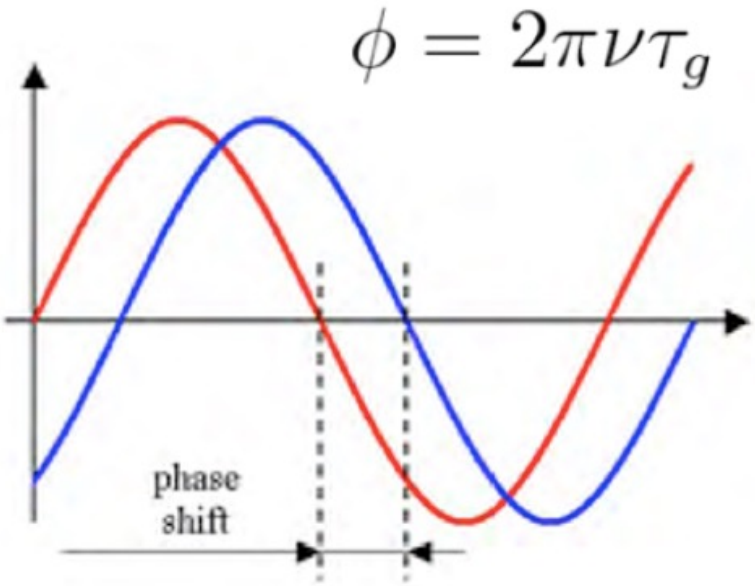

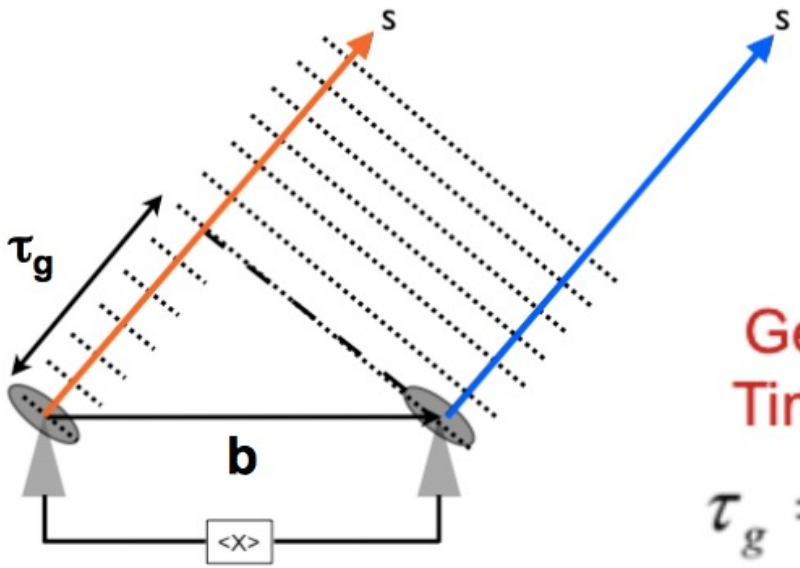

Geometric
Time Delay

$$\tau_g = \mathbf{b} \cdot \mathbf{s} / c$$

The geometric delay that arises from the physical separation of the antennas also has to be factored in.

mm waves

Wavelengths are ~10^3 times greater than IR, and dishes are only a bit bigger (ALMA antennas are 12-m)

The whole wavefront suffers retardation, but analysis by E Archibald et al (2002) found no evidence for beam broadening due to seeing at the 15-m JCMT on Mauna Kea

Anomalous refraction can lead to image excursions, possibly due to large scale cells moving over the site

ALMA does not seem to suffer from this, probably because the PWV is lower on Chajnantor

ALMA Phase correction

- Water vapour in the troposphere is not well mixed, leading to large variance of total water vapour column along different lines of sight through the atmosphere
- Water vapour is usually described in terms of the column of precipitable water vapour (PWV) above the antenna. The PWV at zenith can vary by a factor of 2 above the ALMA site by as much as 50% over a few minutes
- Water vapour has a high effective refractive index, and 1mm of PWV retards the incoming wavefront by about 7mm of path. This is 20λ at ALMA's highest observing frequency
- Radiometers monitor the emission from the 183GHz water vapour line along the line of sight of the observations, providing estimates of the PWV above each antenna.

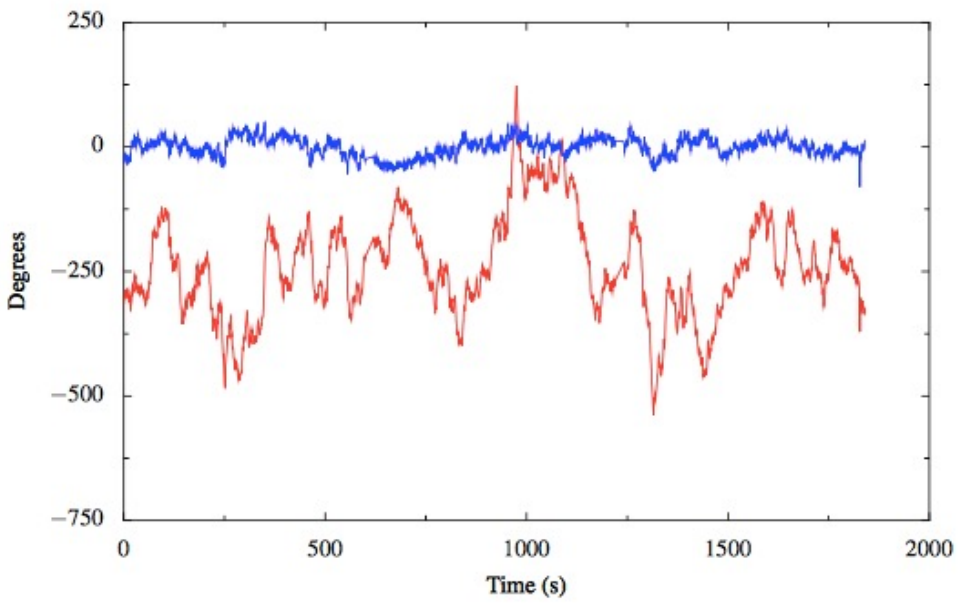

Fig. 8. Test observation at 90 GHz of a strong quasar on a ~650 m baseline with ALMA. The red line is the phase of the observed (complex) visibility on this baseline – note that for a quasar (or other point-like) source at the tracking centre of the interferometer we expect a constant phase in time. The blue line is the visibility phase after correction of the data based on the WVR signals and using the `wvrgcal` program.

Nikolic et al 2013

Space

In space, there is no need to compensate for the atmosphere!!

Diffraction-limited optics take full advantage of unaberrated wavefronts to yield exquisite image quality and sensitivity.

This places severe constraints on the pointing and stability of spacecraft and its payload.

But

Note that the ISM is partially ionized and variations in refractive index can lead to dispersion, scattering and angular broadening at radio frequencies

Atmospheric Seeing

Wavefronts from distant objects are assumed to be plane-parallel, but as the waves propagate through cells in the atmosphere with refractive index variations, they become distorted

The atmosphere changes on short timescales (msec), producing a time- variable distortion. The distortions increase with increasing airmass, i.e. as the elevation of the target decreases, but can also depend on windspeed and direction.

At visible wavelengths this leads to blurring, termed atmospheric seeing, with an image diameter of ~0.5 arcsec under the best conditions at the best sites, compared to the diffraction limit of ~0.015 arcsec for an 8-m telescope

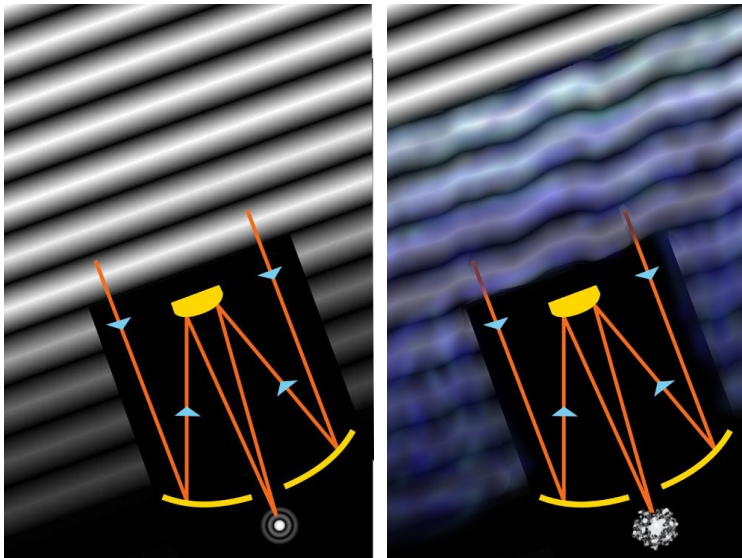

Single Telescope Resolution

- Ultimately, diffraction imposes a limit on the resolution that can be achieved : FWHM = 1.2 λ / D for an unobscured pupil, generally expressed in arcseconds
  - where 1 arcsec = 4.8 x 10^{-6} radians
- The actual resolution achieved depends critically on the atmospheric conditions at visible and near-IR wavelengths.
- At sufficiently long wavelengths (e.g. in the mid-IR), diffraction may be the dominant component of the image size
- In practice image quality may be limited by windshake, tracking errors, misalignments and aberrations, but the lowest orders can be corrected by shift and add or tip-tilt.

Seeing

The corrugations in the wavefront caused by refractive index variations as it propagates through the atmosphere leads to image formation through a set of effective apertures on the scale of the coherence length rather than the full telescope diameter.

The image size is then given by λ/r_o rather than λ/D

At the best sites and conditions, the characteristic scale r_0~ 20cm at a wavelength of 500nm; this corresponds to an image size of ~0.6 arcsec

The overall tilt of the wavefront causes the centroid of the image to be displaced - image wander

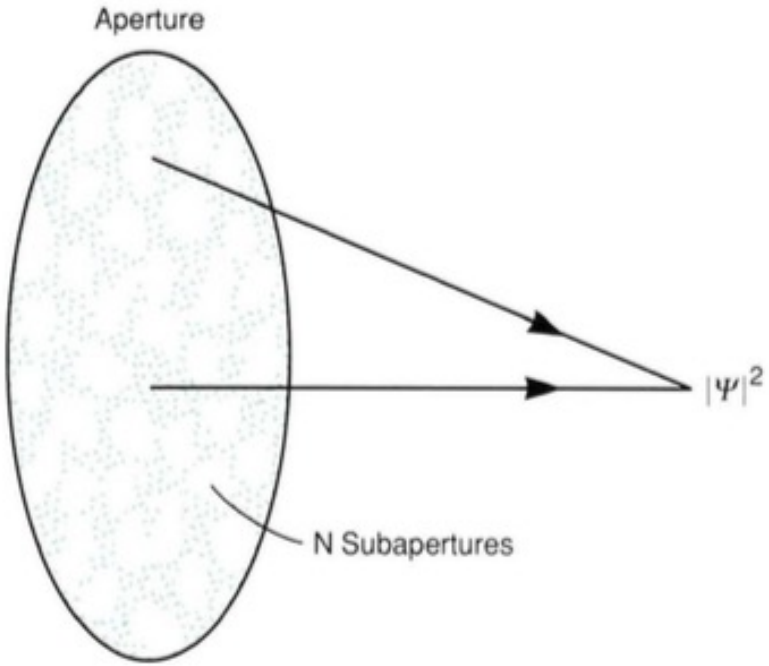

$$|\Psi|^2 = \sum_{i=1}^{N} |\Psi_i|^2 + \sum_{i \neq j} \sum_{j} \Psi_i \Psi_j^*$$

	Seeing Disk	Sum of Uncorrelated Random Phasors
Applicable Spatial Frequencies	Low	High
Intensity ~	N	$N^{1/2}$
Power ~	N^2	N
Normalized Power ~	1	$1/N$

Fig. 1—The division of the telescope aperture into N *effective subapertures. The image results from two independent terms with different dependences on* N. *The first term describes the superposition of the intensities of all the individual subapertures, and the second term describes the interference between the subapertures.*

Telescope Image

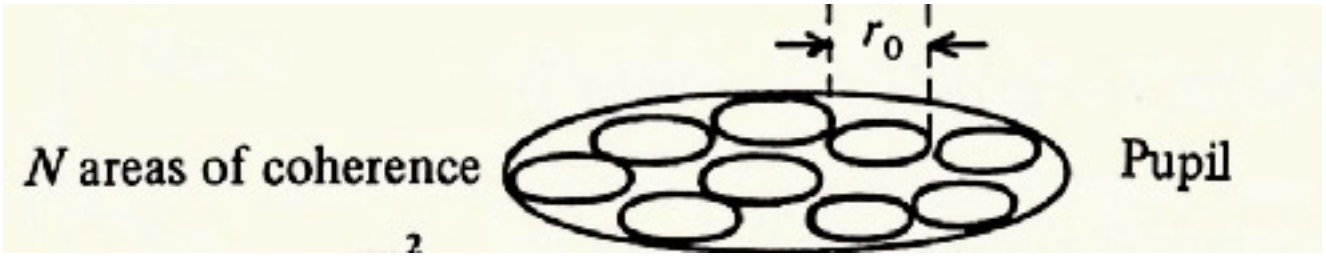

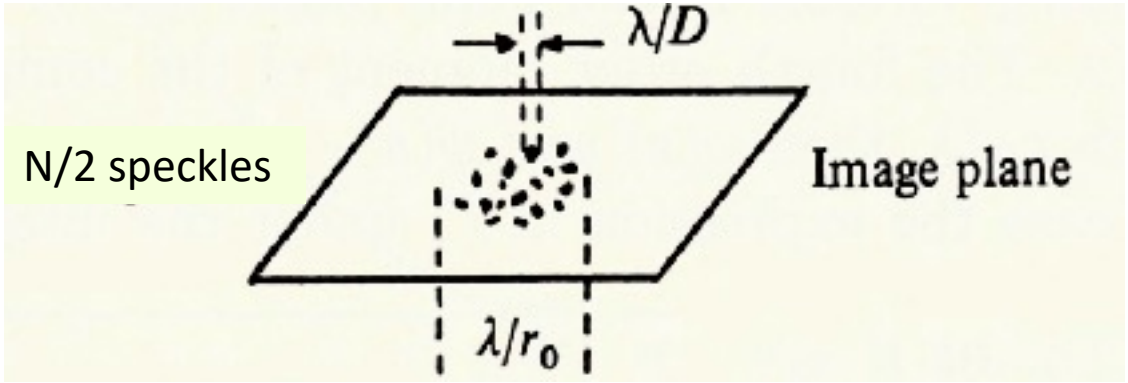

The telescope pupil contains $N= (D/r_0)^2$ cells of diameter r_o, which produce speckles of size ~λ/D within the envelope given by the diffraction pattern on a scale λ/r_o

Seeing

- Short exposures (few msec) freeze the effects of the atmosphere providing snapshots of the distorted image, which shows a blurred core with ‘speckles’.
- Long exposures average over the variations, providing a blurred image characterized by the “seeing disk”.
- The 14 arcsec double star 100 Her sampled at 10 msec frame rates (C MacKay)
- Note the good correlation in the gross motion of the two images

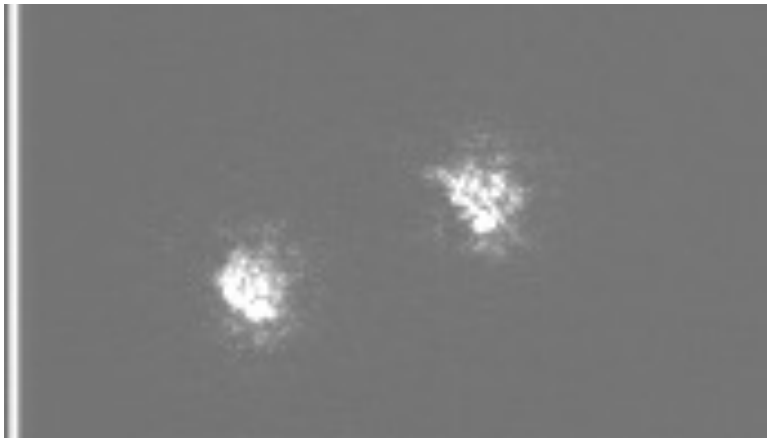

Image distortions

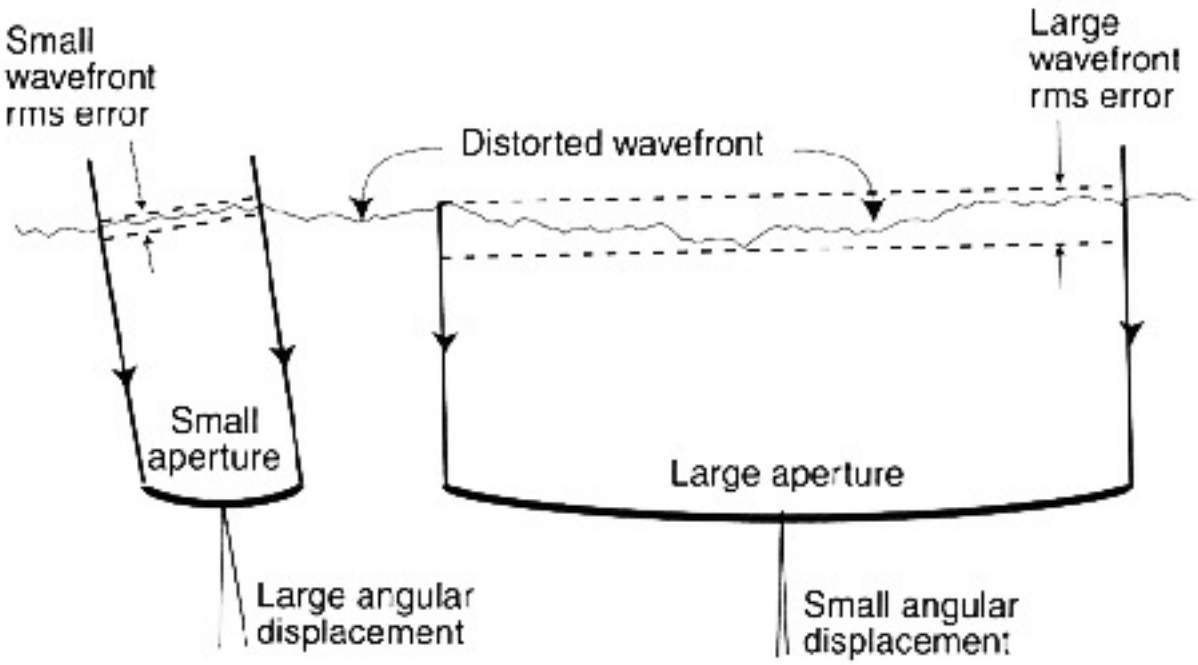

When the telescope aperture is similar to r_o , the dominant distortion will arise from tilts in the wavefront, causing image wander.

Larger apertures encompass many r_o and so the image will be the sum of many images blurred on a scale of λ/r_o randomly displaced by the wavefront tilt in the subaperture.

Tip-tilt correction applied to the telescope secondary can (partially) compensate for the overall wavefront tilt, and so is effective at mid-IR wavelengths on 8-m telescopes, near-IR on 4-m telescopes and amateur scale telescopes in the visible.

Similar improvements can be made by using burst mode- many short exposures that are shifted and added, discarding any poor quality images.

Or by using “Lucky Imaging”, selecting only the highest quality images for coaddition. Both of these techniques impose significant overheads on the observations.

(Figure from Bely)

Strehl Ratio

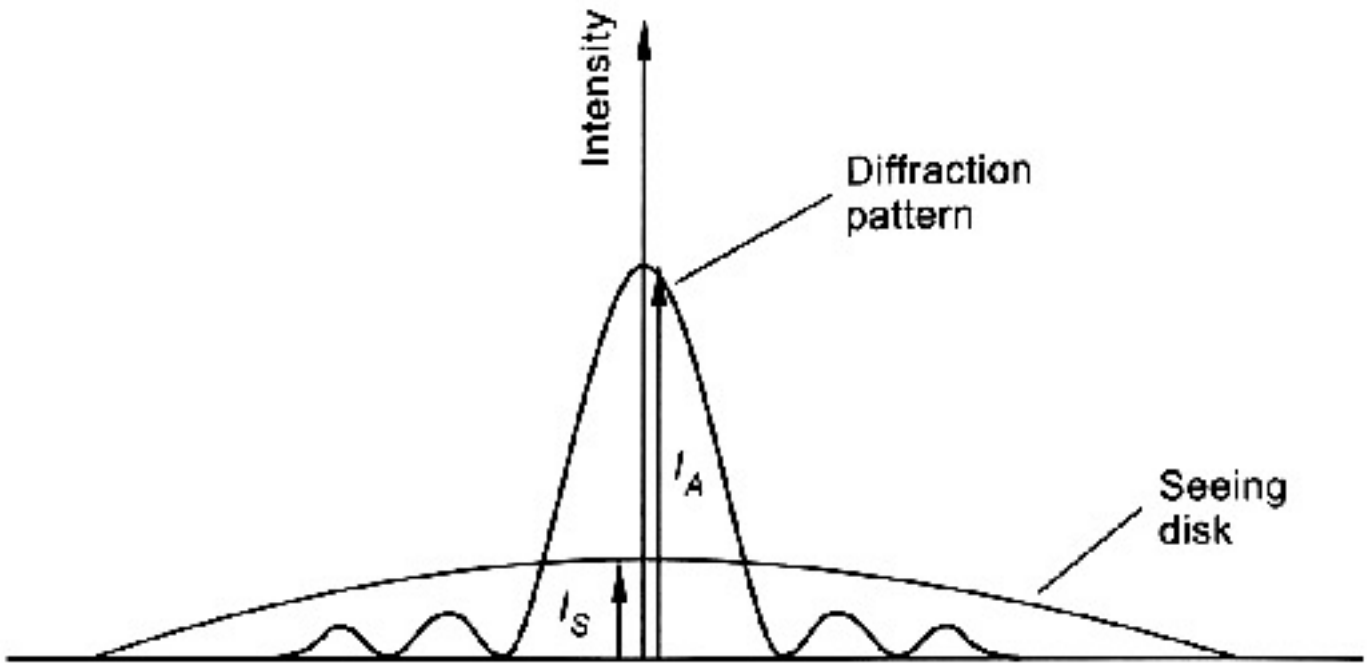

The ratio of the peak intensity of the measured image to that calculated from the diffraction pattern of the telescope optics is the Strehl Ratio

Wavelength dependence

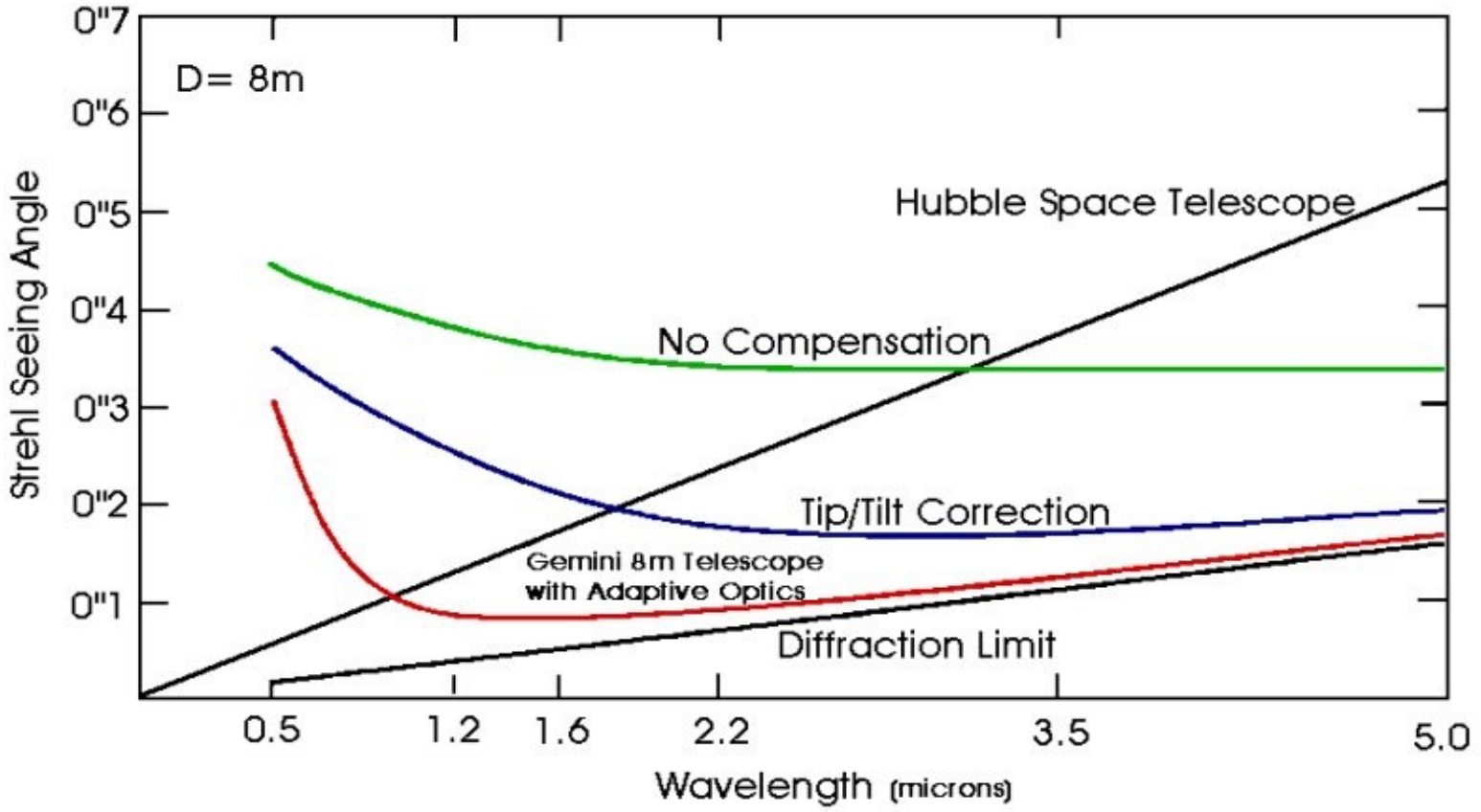

- To a good approximation, atmospheric turbulence follows a Kolmogorov spectrum, with the coherence scale

  $r_0(\lambda) \sim r_0(\lambda_0)\,(\lambda/\lambda_0)^{1.2}(\cos(z))^{0.6}$.

- so that the seeing disk in the IR is smaller than in the visible : FWHM $\alpha\ \lambda^{-0.2}$
- At 2µm it is 0.75 times that at 0.5µm, and at 10µm it is 0.55.

Effect of the Telescope Central Obstruction

pushes more power into the diffraction rings, but also narrows the central maximum

It also reduces the flux collected and produces greater discontinuities in the wavefront in the telescope pupil

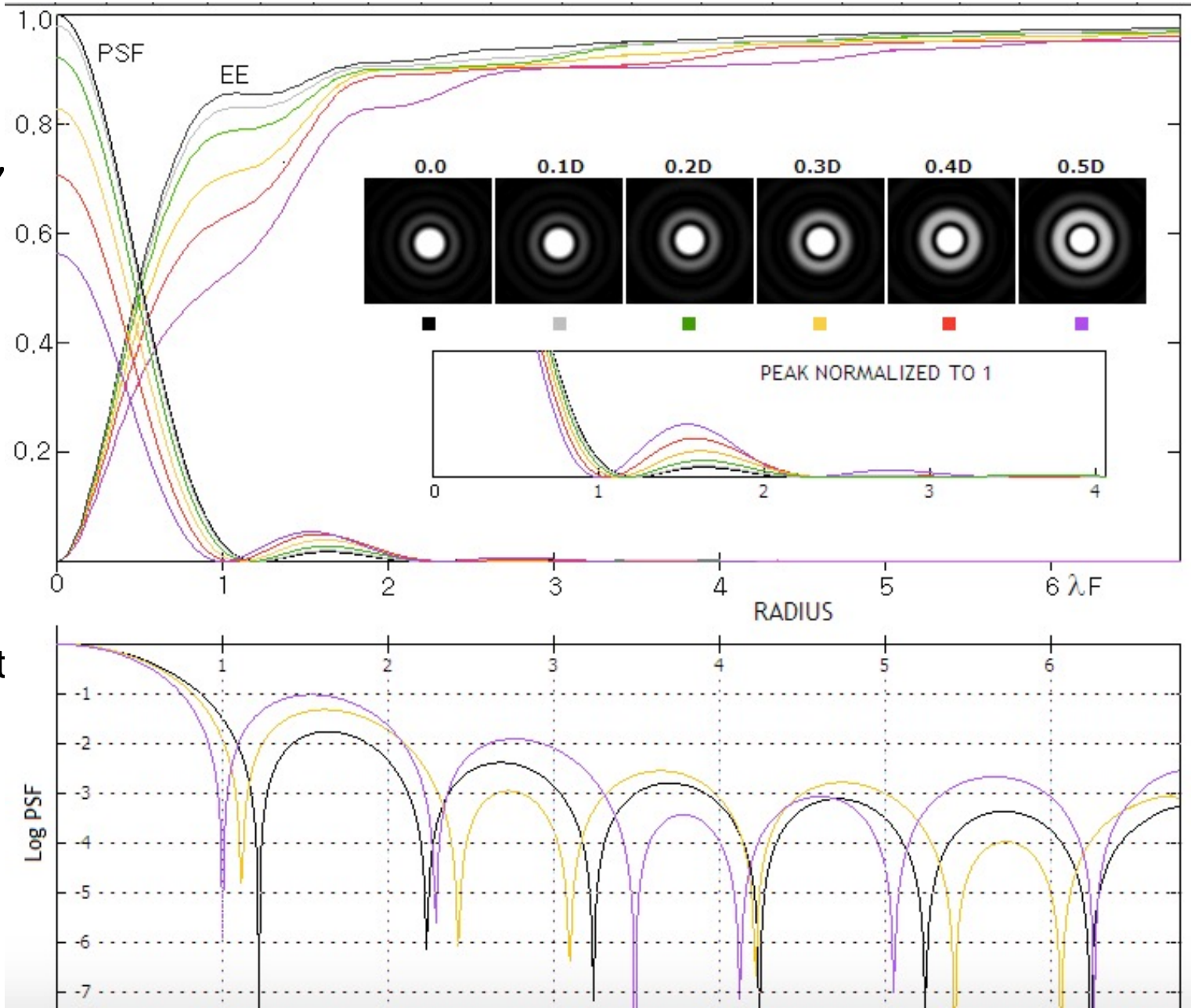

- The point spread function delivered by the telescope depends on the mirror surfaces and alignment, the atmosphere and the effects of the central obstruction and secondary mirror vanes on the telescope pupil.

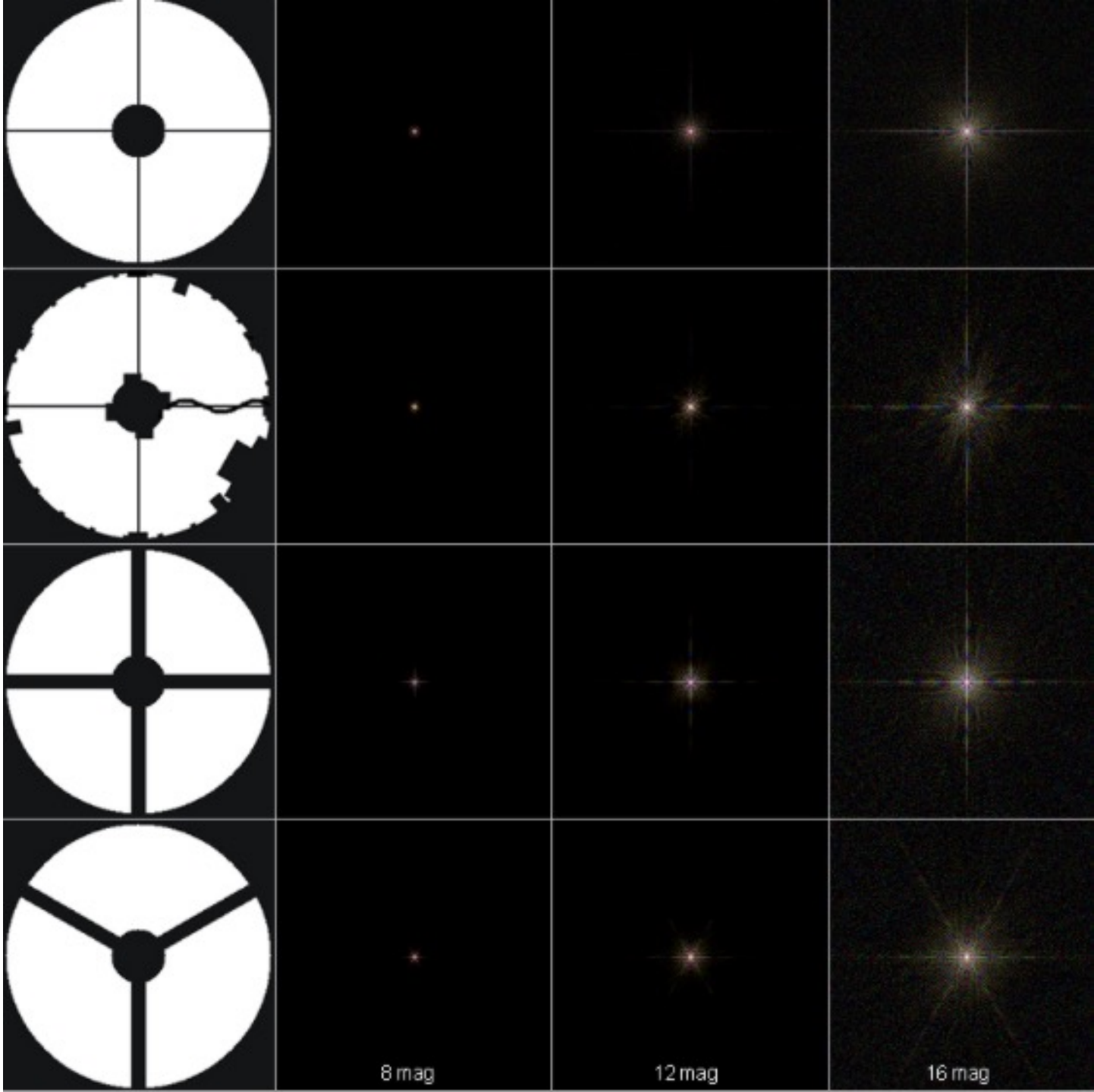

R Pascal

Seeing

- Turbulence along the whole path through the atmosphere contributes to the seeing
  - Jet stream can produce very fast winds, rapid changes and short coherence times
  - Local heating or topography from the mountain or the telescope dome can generate additional turbulence over the free-air profile - ground layer turbulence
  - Seeing may be seasonal or depend on wind directions etc

Many sites monitor seeing in real time using a DIMM (Differential Image Motion Monitor), but for accurate measurements the DIMM should be colocated and at the same altitude as the primary mirror

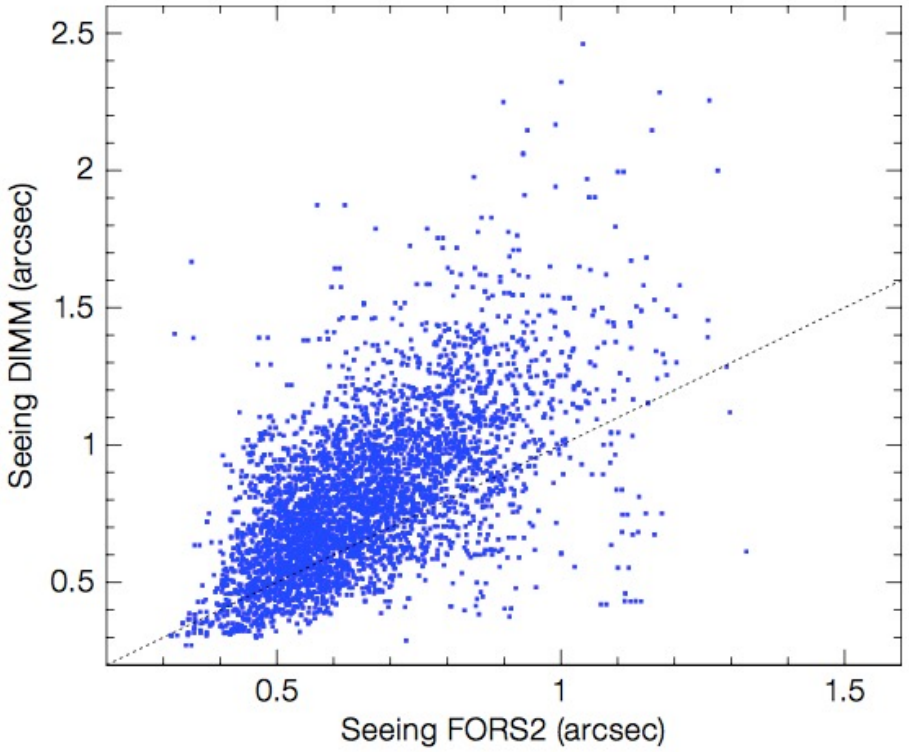

Seeing at Paranal

The DIMM measurements at Paranal are affected by a ground layer of turbulence that becomes prominent when the wind blows from the NNE or SSE.

This layer does not affect the VLT images, as M1 lies above it.

The wind rose plots the discrepancy between DIMM and UT1 seeing as a function of wind direction

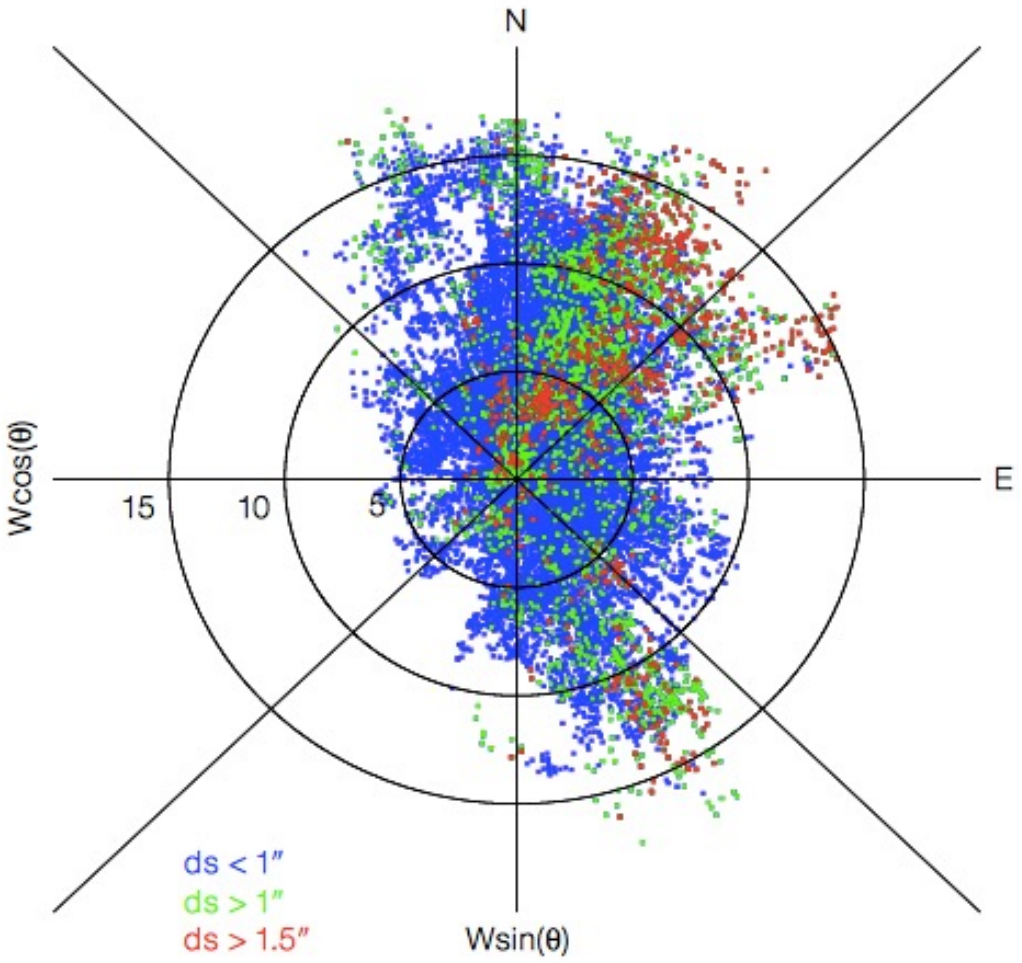

Coherence time

- The simplest model assumes that the turbulent atmosphere is blown across the telescope aperture by the wind.
- In this case, the characteristic (Greenwood) frequency of the atmosphere can be approximated by:
- $f_G = 0.43\ V_{wind}/r_0$ which, with $r_0 \sim \lambda^{1.2,}$ means that the coherence time, $t_0 \sim \lambda^{1.2}$ and is in the range ~2 to 20msec from the visible to the IR.
- The frame time to freeze the atmosphere is longer at IR wavelengths while the number of r_0 subapertures in the telescope pupil is smaller
- At long wavelengths, r_0 can approach the size of the telescope aperture and low order correction will be effective. At shorter wavelengths, higher order correction – Adaptive Optics – is required.

Shift and Add can sharpen images

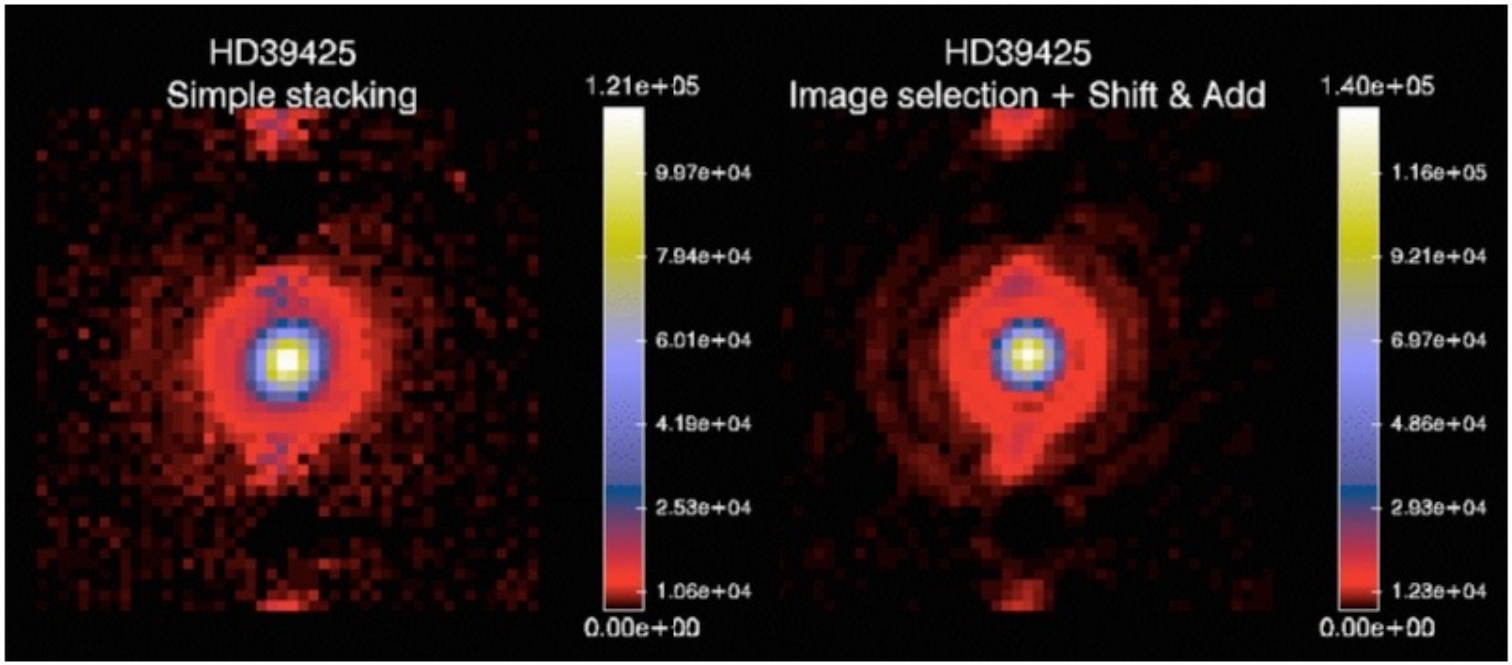

Figure 5. Left panel : simple stack of burst mode frames of the standard star HD39425, simulating a classical observation. Right panel, shift-and-add and image selection are applied to burst mode data. The average FWHM is decreased by 15% and the Strehl ratio is improved from 0.52 to 0.65. Note also the two unveiled diffraction rings (dark red) appearing in right panel.

Images with VISIR on the VLT demonstrate the improvements obtained with shift and add

Effects of atmospheric turbulence - seeing

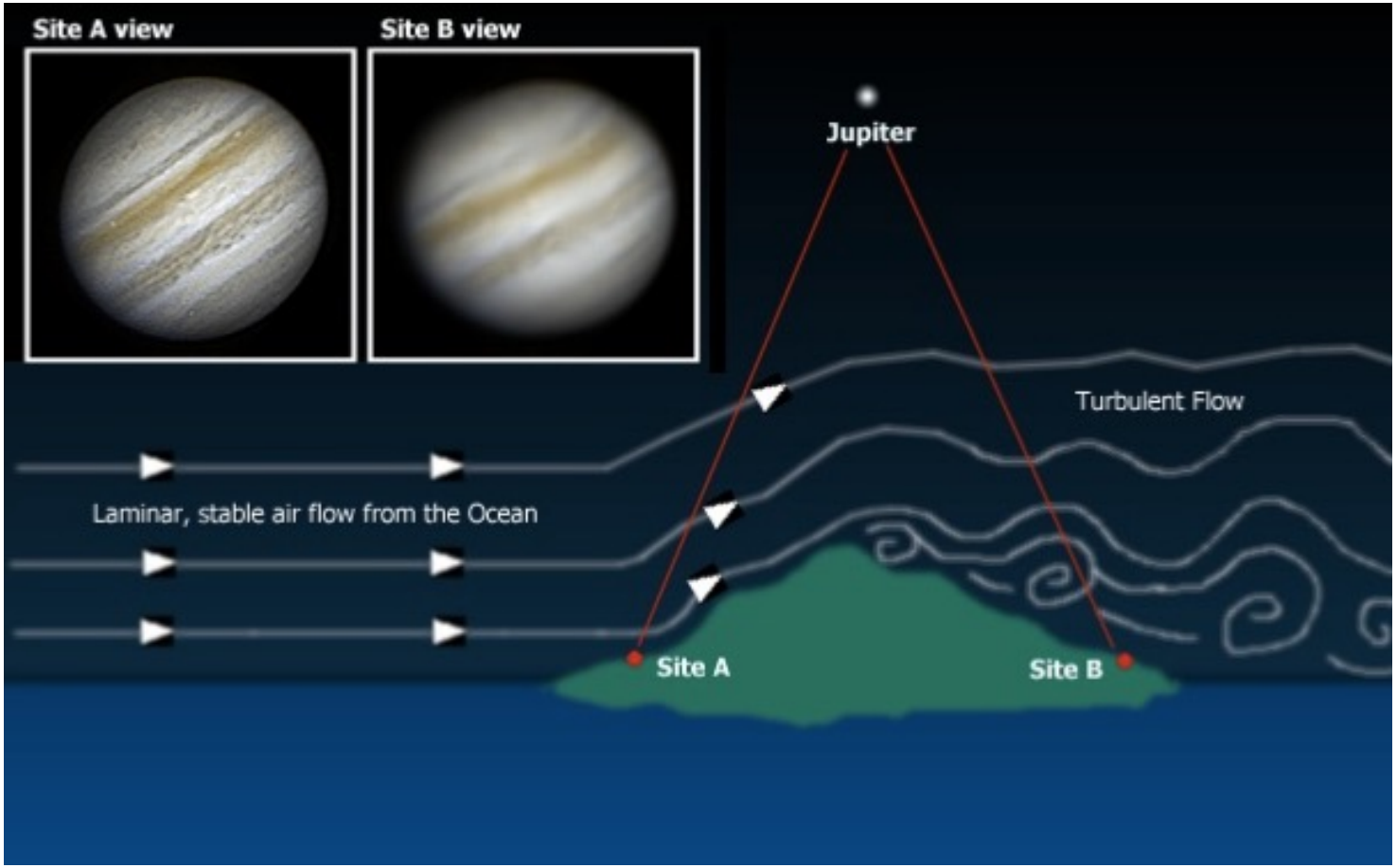

Seeing-limited images

- In long exposures, the speckle component averages out, and the resultant image is the accumulated integration of the images of size λ/r_0
- The resulting images typically have a near-gaussian core set by the transfer function of the atmosphere.
- However at large angles (>5arcsec), scattering from mirror imperfections (scratches, splodges etc) lead to a halo which is brighter than expected for diffraction alone.
- Note that because of the wavelength dependence of seeing, stars of different colours will have slightly different profiles in wide-band images.

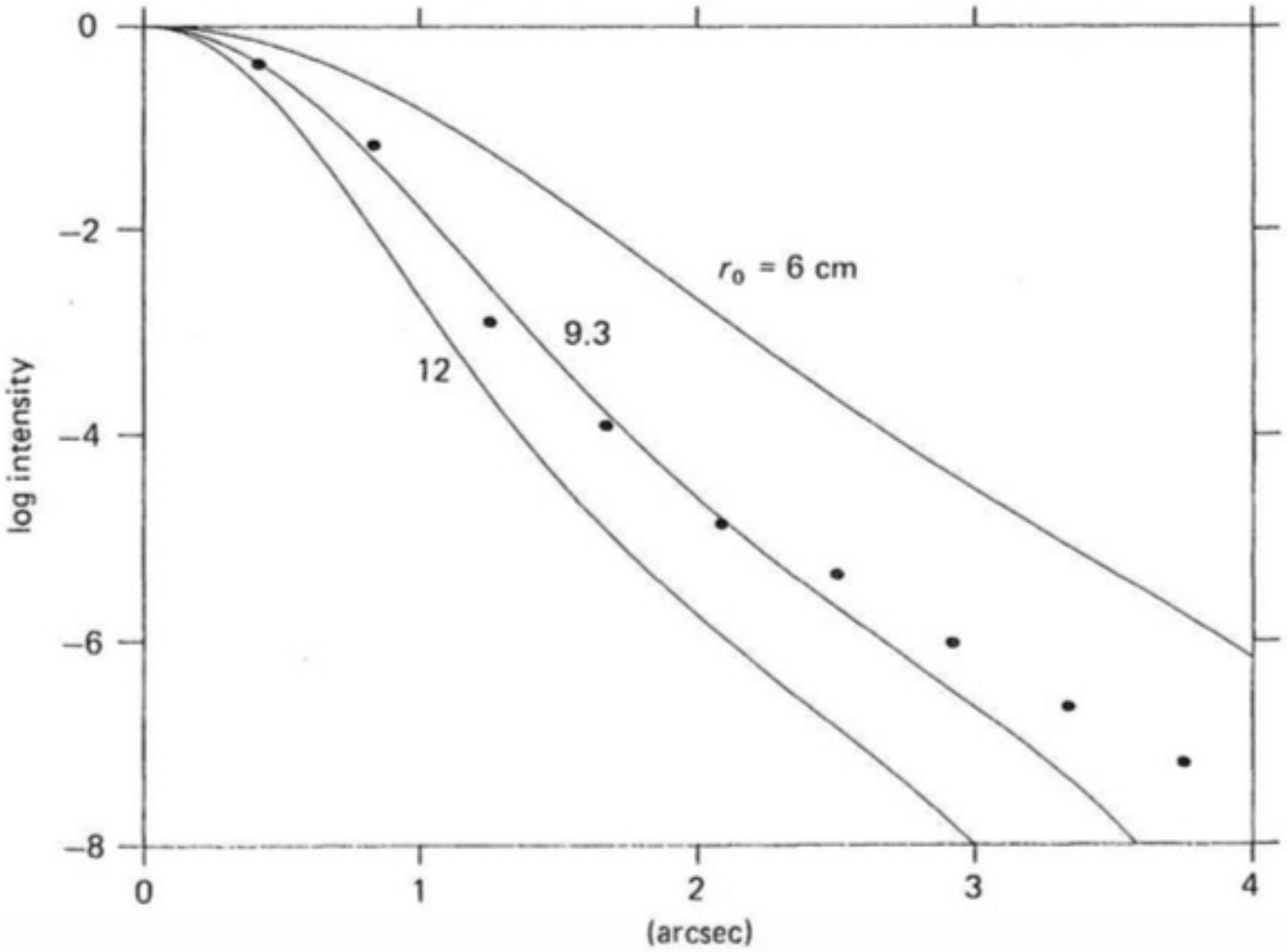

Theoretical long exposure image profiles for 3 different values of r_0 compared with observations (points) made in average seeing conditions at V with the CFHT on Mauna Kea The departure beyond 3 arcsec probably represents the mirror scattering component (G Walker 1989)

Achieving high resolution

- Diffraction-limited performance with single telescopes with Adaptive Optics
- Or sparse aperture masking
  - Use masks to sub-divide telescope primary into a number of subapertures which are combined interferometrically
  - http://www.eso.org/sci/publications/messenger/archive/no.146-dec11/messenger-no146-18-23.pdf
- Interferometry with 2 or more separated telescopes where the resolution depends on λ/b where b is the maximum baseline between apertures
- Plus: lunar occultations, speckle interferometry....

Adaptive Optics

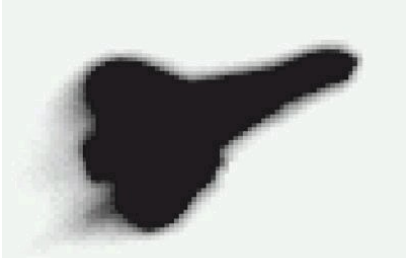

The Space Shuttle imaged with AO from the Starfire Optical Range, Phillips AFB, NM

Proposed by Horace Babcock in 1953.
"The Possibility of Compensating Astronomical Seeing"

Developed by US military for satellite observations from the ground, and laser beam propagation.

Astronomical developments in the 1990s as control systems evolved.

Now important in medical imaging and microscopy:

Imaging and spectroscopy of the retina, lens and cornea:

Diagnosis of diseases of the eye
- **Diabetic Retinopathy**
- **Macular degeneration**
- **……**

Window into the circulation and nervous system